SECTION I

RESEARCH IN PROGRESS

NUCLEAR STRUCTURE -- EXPERIMENTAL

β-DELAYED NEUTRON SPECTROSCOPY

R. Harkewicz, K. McDonald, D.J. Morrissey, and J. A. Nolen, Jr.

A neutron time-of-flight spectrometer has been developed to study neutron emission from the exotic nuclei newly available from the A1200 separator. This device relies on the unique ability at the NSCL to transport beams of radioactive ions to low background counting environments and to implant these ions in a particle telescope. Beta-delayed neutron emission is an important decay mode of very neutron rich nuclei and a large number of studies of the total neutron emission probability have been performed. However, relatively few detailed spectra have been obtained due to the difficulties associated with neutron spectroscopy. We have developed a broad range neutron spectrometer based on determination of the neutron energy by time-of-flight (TOF) measurements with plastic scintillators. A very efficient start signal can be obtained from the beta-particle when the decaying nuclei are implanted in the middle of a charged particle detector and moderate neutron efficiencies can be obtained with large plastic scintillators.

A schematic diagram of the neutron array is shown in figure 1. The beam of radioactive ions

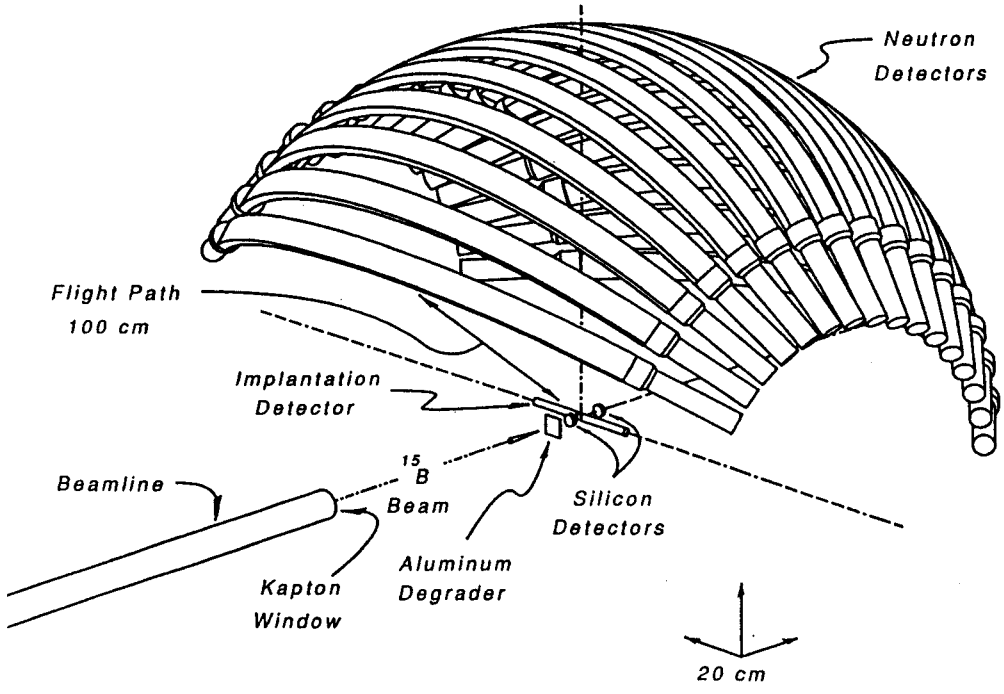

Figure 1: Neutron array.

passed through a thin Kapton window that separated the beam-line vacuum, then approximately 1m of air, an aluminum degrader, a thin silicon surface barrier detector and came to rest in the center of a

plastic scintillator. A second silicon surface barrier detector was placed behind the implantation detector to identify more pepetrating particles. The combination of energy loss in the first silicon detector with TOF versus the cyclotron rf signal allowed on-line monitoring of the number and type of implanted particles. The inplantation detector was partically surrounded by 16 large area (157 cm by 7.6 cm by 2.54 cm thick) BC412 plastic neutron detectors, each bent is a 1 m radius. Neutrons leaving the centered source and interacting with the neutron detectors would have a uniform pathlenght of 1 meter. The 16 detectors covered a solid angle of approximately 1.9 sr. Each neutron detector and the central implantation detector was connected to two photomultiplier tubes so that the mean-time of each event cound be determined. A typical efficiency for detecting a beta particle in the central detector was 80% and for observing a 1.0 MeV neutron in a slat was 20%. Details of the calibration and operation of the device have been given by Harkewicz [1].

In the first experiment [2], the nTOF spectrometer was tested and then used to study the spectrum of neutrons emitted after the β- decay of ^{15}B. The intensity and purity of ^{15}B ions was sufficently high (approximately 600/sec at 94% purity) that the cyclotron beam was cycled on and off and neutrons were observed during the beam-off period. Typical on and off periods were approximately 20 and 40 ms, respectively. The halflife was remeasured and a very weak branch to neutron bound states was observed with the inclusive beta particles. A neutron TOF spectrum from one of the sixteen array elements is shown in figure 2. A peak resulting from relativistic electrons that traveled from the implantation detector to the slat (i.e., from the β-decay of ^{15}B) appeared in channel 186.6, not shown in this figure, and provided a reference for the neutron TOF. The areas of the peaks were fitted and combined with the detector efficiency gave the beta-decay branching ratios.

Following its inauguration, the device was used in collaboration with several outside user groups to study neutrons from a number of light nuclei. A group from the University of Notre Dame began a series of measurements of light neutron-rich nuclei that are important in the astrophysical r-process [3]. The goal is to determine the beta-delayed neutron branching in heavy carbon, nitrogen and oxygen nuclei in order to determine the path of neutron capture. An independent calibration of the neutron efficiency was obtained by measuring the decay neutrons from ^{17}N followed by a study of the neutrons from ^{18}N. Another group from the University of Notre Dame used the nTOF array in concert with several gamma-ray detectors to study the beta decay of ^{14}Be [4]. And most recently, several scientists from Russia visited MSU

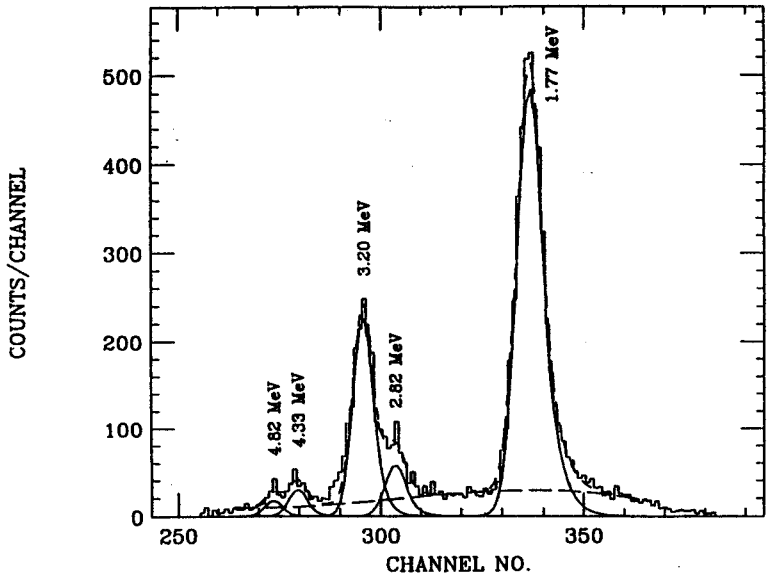

Figure 2: TOF spectrum

to work on measurements of multiple neutron decay from ^{11}Li [5].

References

1. R. Harkewicz, Ph. D. Thesis, Michigan State University, 1992.
2. R. Harkewicz, *et al.*, Phys. Rev. C44 (1991) 2365.
3. J. Görres, M. Wiescher, and K. Scheller, University of Notre Dame.
4. M. Belbot, J. Kolata, K. Lamkin, R. Tighe, and M. Zahar, University of Notre Dame.
5. G. Chubarian, S. Lukyanov, and Yu. Oganessian, Joint Institute for Nuclear Reactions, Dubna.

MOMENTUM DISTRIBUTIONS OF ^{9}Li FRAGMENTS FOLLOWING THE BREAKUP OF ^{11}Li

N.A. Orr, N. Anantaraman, Sam M. Austin, C.A. Bertulani [a], K. Hanold [b], J.H. Kelley, D.J. Morrissey, B.M. Sherrill, G.A. Souliotis, M. Thoennessen, J.S. Winfield, J.A.Winger

We have undertaken a series of measurements of the parallel momentum distributions of ^{9}Li fragments from the breakup of a ^{11}Li beam. To make these measurements the A1200 fragment separator was operated for the first time as an energy loss spectrometer.

Previous studies of ^{11}Li have indicated that the very weak binding of the valence neutrons (S_{2n} = 0.34 ± 0.05 MeV[1]) may result in a neutron distribution extending well beyond that expected from systematics - the so-called "halo". In particular, a study at LBL[2,3] which measured the transverse momentum distributions of products from the fragmentation of ^{11}Li found a very narrow structure in the ^{9}Li spectrum ($\sigma_{\perp}$ = 21 ± 3 MeV/c) from breakup on a carbon target. In simple terms this may be related by the uncertainty principle to a large spatial distribution of the stripped neutrons.

An important issue in the present study was to understand whether the momentum distributions reflect only the structure of ^{11}Li or are also dependent on the interaction governing the breakup process. One means of answering this question is to perform measurements on heavy nuclei in order to compare results for Coulomb induced breakup to data for low Z targets, where the breakup is presumably mediated by the nuclear interaction. However, for reactions on heavy nuclei, transverse momenta are strongly affected by Coulomb deflection[4] and multiple scattering in the (relatively thick) breakup targets. These effects precluded any possible observation of a narrow structure in the transverse momentum distributions when a lead target was used, where a width of $\sigma_{\perp}$ = 71 ± 15 MeV/c was measured[2]. Furthermore, transverse momentum distributions measured in the breakup of weakly bound nuclei have been shown to be sensitive to diffractive broadening[5]. In contrast, the parallel momentum distributions are not perturbed by these effects.

The major problem encountered in making the measurements using the ^{11}Li secondary beam was its large energy spread as it was produced by the fragmentation of a ^{18}O primary beam (80 MeV/nucleon) in a thick (790 mg/cm^2) beryllium target. To obtain the necessary final resolution despite the large spread in energy of the ^{11}Li ions, the A1200 was employed as a zero degree energy loss spectrometer operated in a dispersion matched mode[6]. This mode of operation allowed the full 3% momentum acceptance ($\Delta p(^{11}\mathrm{Li}) \approx 120$ MeV/c) of the device to be utilized whilst retaining a final resolution of 0.1%. Since the total momentum is dominated by the parallel momentum, the two are essentially equivalent (under the present experimental

conditions to within 0.02%).

Measurements were made for three different breakup targets (^{9}Be, ^{93}Nb and ^{181}Ta) using the two different optical modes of the A1200 - the "medium" and "high" acceptance modes. Production rates for ^{11}Li of ~10 and ~50pps/pnA of ^{18}O beam were obtained for the two modes respectively and the average energy of the ^{11}Li ions incident on the breakup targets was ~66 MeV/nucleon. The central 2% of the momentum distributions were measured and single Gaussian functions were fitted to the data (as shown for example in figure 1).

Perhaps the most striking feature of the present results, illustrated in figure 2, is the weak dependence on target of the width of the parallel momentum distributions. Kobayashi et al.[7] and Riisager et al.[8] have shown that for heavy targets the dominant reaction process for the breakup of ^{11}Li to ^{9}Li is Coulomb dissociation, whilst for light targets the reaction should proceed almost exclusively by nuclear induced breakup (an effect which appears more pronounced at low energies[8]). Thus, it appears that the nature of the interaction governing the breakup plays only a weak role in determining the parallel momentum distributions of the outgoing ^{9}Li fragments.

A large amount of theoretical work has been undertaken to describe the structure and breakup of ^{11}Li and momentum distributions are predicted by many of the models. For example, the ^{181}Ta target data is compared in figure 1 with the model proposed by Esbensen and Bertsch[9] (shown as a dashed line). This approach incorporates a three-body description of ^{11}Li and dissociation proceeds via Coulomb excitation. As noted earlier, this should be the dominant mechanism for breakup on heavy nuclei. The agreement with the present data is very good.

A more complete description of the present work has been submitted for publication[10]. In future we intend to study more weakly bound systems such as ^{11}Be, ^{14}Be to obtain more complete systematics.

[a] On leave from: Instituto de Fisica, Universidade Federal do Rio de Janeiro, 21945 Rio de Janeiro, Brazil

[b] Nuclear Science Division, Lawerence Berkely Laboratory, Berkeley, CA 94720

References

1. T. Kobayashi et al., KEK preprint 91-22, 1991 (to be published)
2. T. Kobayashi et al., Phys. Rev. Lett. 60 (1988) 2599
3. T. Kobayashi et al., in "Radioactive Nuclear beams 1991", ed. Th. Delbar (Adam Hilger, Bristol, 1992) p197
4. K .Van Bibber et al., Phys. Rev. Lett. 43 (1979) 840
5. C.A. Bertulani and K.W. McVoy, NSCL preprint MSUCL-834, 1992 (to be published)
6. B.L. Cohen, Rev. Sci. Instr. 30 (1959) 415
7. T. Kobayashi et al., Phys. Lett. B232 (1989) 51

8. K. Riisager et al., Nucl. Phys. A540 (1992) 365
9. H. Esbensen and G.F. Bertsch, Nucl. Phys. A accepted for publication
10. N.A. Orr et al., submitted to Phys. Rev. Lett.

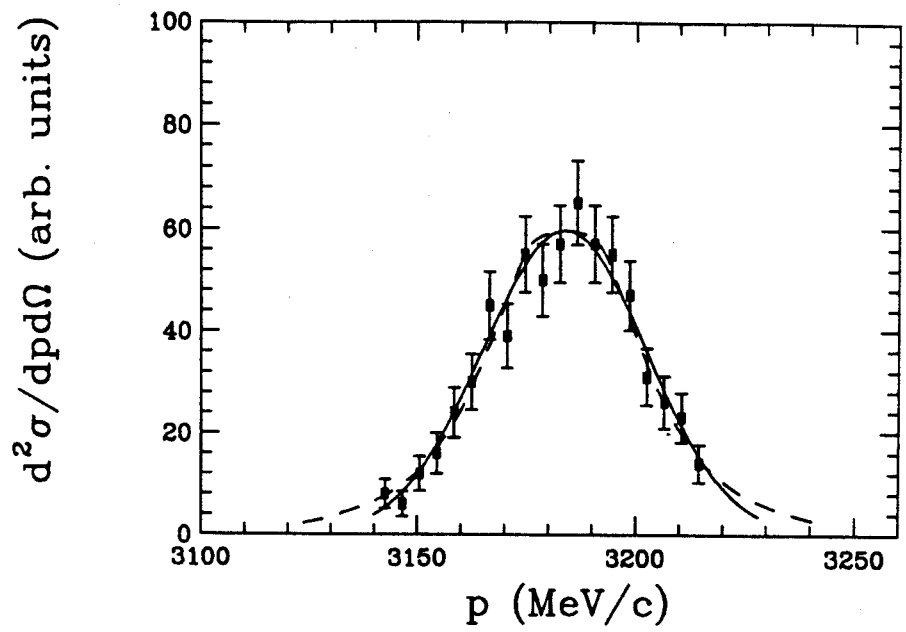

Figure 1 : Momentum distribution covering the central 2% of the breakup ^{9}Li momenta with a single Gaussian fit (solid line) for a high acceptance mode measurements using the ^{181}Ta target. The dashed line shows the prediction of Esbensen and Bertsch[9].

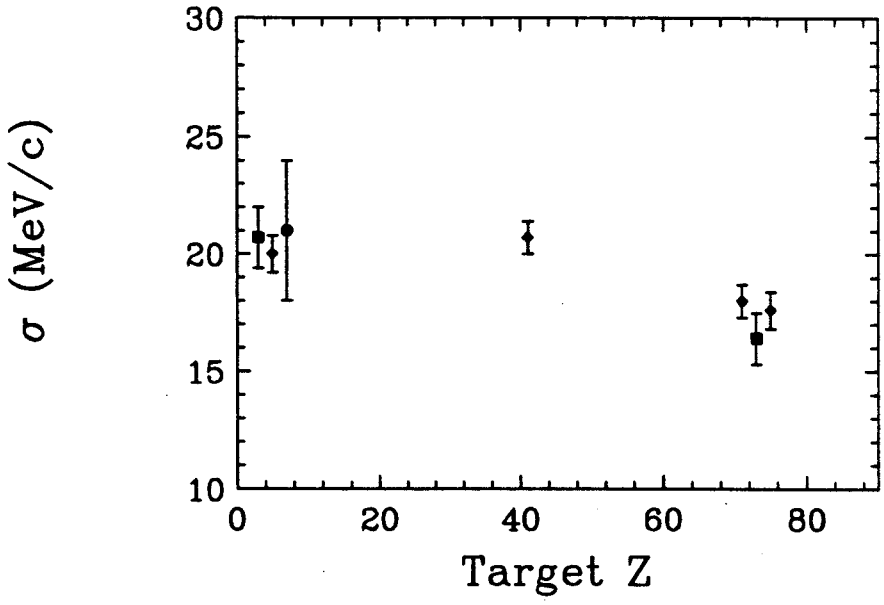

Figure 2 : Target Z dependence of the widths (Table 1) of the momentum distributions for the medium (squares) and high (diamonds) acceptance mode measurements. The result of Kobayashi et al.[2] is indicated by the circle.

STUDY OF THE $^{13}C(^{13}N,^{13}C)^{13}N$ MIRROR CHARGE-EXCHANGE REACTION AT E/A = 57 MeV/u

M. Steiner, W. Benenson, C. Bertulani, E. Kashy, R. A. Kryger, N. A. Orr, B. M. Sherrill, M. Thoennessen, S. J. Yennello, and B. M. Young

The exchange of mesons — and in particular pions — between nuclei is of fundamental importance since they mediate the nuclear force. Charge-exchange reactions between mirror pairs of nuclei offer a new possibility to study the long-range part of the nuclear pion field since at 0°, they occur with zero momentum transfer and hence should be sensitive to pion exchange at large impact parameters. A good candidate for the investigation of charge exchange between mirror nuclei is the reaction $^{13}C(^{13}N,^{13}C)^{13}N$, since ^{13}C targets are available and a relatively intense ^{13}N beam can be produced.

The goal of the experiment was to measure the differential reaction cross section $d\sigma/d\Omega$. We compare it to a model calculation [1] which describes heavy-ion charge-exchange reactions in the eikonal approximation, taking into account the contributions of π– and ρ–meson exchange.

We have performed this experiment operating the A1200 beam analysis device in dispersion-matched mode [2] . The radioactive ^{13}N beam was produced in a 400 mg/cm^2 thick beryllium target by fragmentation of ^{14}N ions with an incident energy per nucleon of 70 MeV. We obtained a rate of approximately 3×10^5 ^{13}N ions per second with E/A = 57.1 MeV. The horizontal angular acceptance of the A1200 was limited to $\pm 0.5°$. Secondary reaction products were identified at the focal plane using the ΔE and total–energy signals from an ion chamber and a thick plastic scintillator, respectively. Position and angle were recorded with two parallel–plate avalanche counters.

The reaction target, with a thickness of 13 mg/cm^2 and made up of equal amounts (by weight) of ^{13}C and ^{12}C, was inserted at the image 2 position of the A1200. The magnetic field strength of all magnets from the image 2 to the focal plane was then increased by one sixth to accomodate the stiffer ^{13}C ions from the charge exchange. ^{13}N particles with the charge state 6+ — which constitute a fraction of about 10^{-5} of the secondary beam — also arrive at the focal plane and served to calibrate the position and shape of the ^{13}C peak. Small variations arising from the slightly different energy loss, straggling and angular scattering of ^{13}N and ^{13}C particles in the target were accounted for with the help of numerical calculations. The number of $^{13}N^{6+}$ ions for each run is also used for normalization, together with the information from four beam current monitors measuring the rate of particles scattering off the production

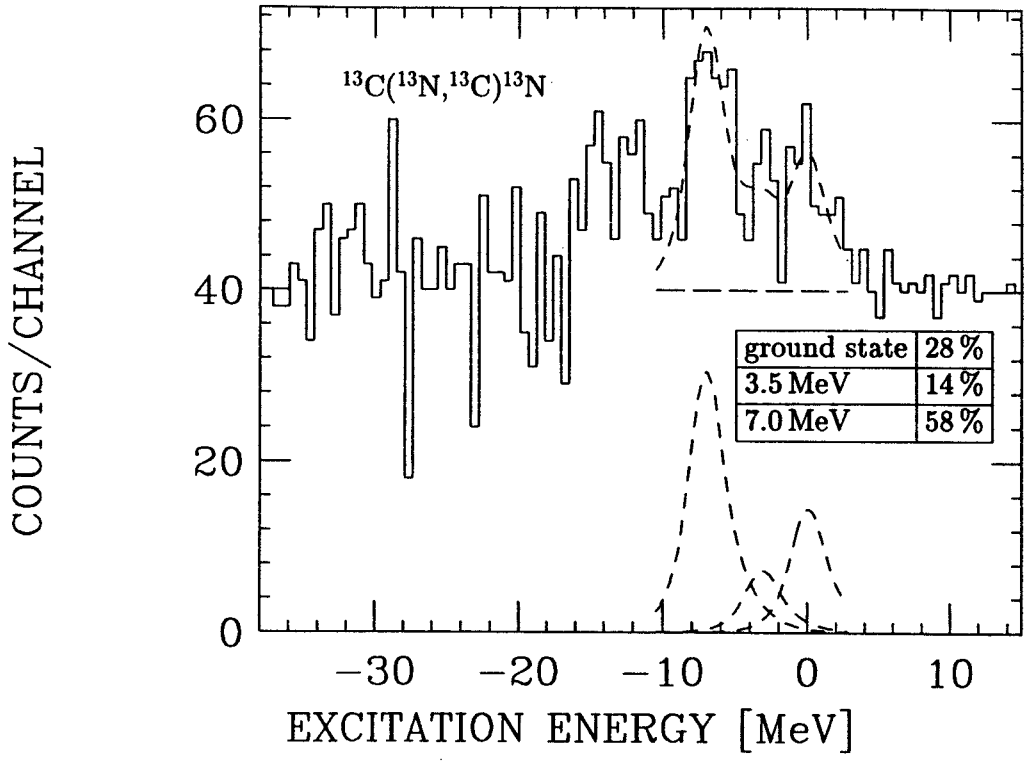

Figure 1: Energy spectrum of ^{13}C from $^{13}C(^{13}N,^{13}C)^{13}N$, taken at the focal plane of the A1200. To correct for background, data taken with a target of natural carbon have been subtracted.

target. To correct for background arising from scattered primary beam and from reactions with ^{12}C nuclei in the secondary target, a background measurement was performed with a ^{12}C target of equal thickness. Figure 1 shows the position spectrum of ^{13}C at the focal plane after addition of a pedestal of 40 counts per channel and background subtraction. The position of the ground–state ^{13}C peak is determined by simultaneous measurement of the $^{13}N^{6+}$ peak position. The dashed curve is a fit assuming that ^{13}C ions can leave the target in the ground state, with eithe r projectile or target nucleus excited to their lowest state at 3.5 MeV, or with both nuclei excited to that state. The relative strengths found for these three states are given in the figure.

The total cross section for the ground–state charge–exchange reaction is $\sigma_T = (17 \pm 7)\,\mu$b, assuming that the distribution is strongly forward–peaked. This value is about a factor of 2 larger than predicted by reference 1. Data analysis to obtain the differential cross section is still in progress.

References

1. C. Bertulani, subm. for publ. in Nucl. Phys. A.
2. H. G. Blosser et al., NIM 91 (1971) 61.

COLLINEAR FRAGMENT-PROTON COINCIDENCE MEASUREMENTS IN FRAGMENTATION REACTIONS AT 0°

A. Azhari, W. Benenson, R. A. Kryger, D. J. Morrissey, N. A. Orr, E. Ramakrishnan, B. M. Sherrill, M. Thoennessen, J. A. Winger, S. Yokoyama, and B. M. Young

The determination of the proton drip-line is still of high current theoretical interest, and the masses and lifetimes of proton unstable nuclei which are located along the drip-line are unique tests for nuclear structure calculations. So far only four ground state proton emitters have been directly observed in the medium mass region.[1] The masses of proton unstable nuclei in the lower mass region were determined from Q-value measurements.[2] Extending proton decay measurements to nuclei of extremely short lifetimes ($\sim 10^{-21}$s) will yield detailed information on nuclei beyond the proton drip-line.

We applied the method of sequential proton decay spectroscopy to measure the mass and lifetime of proton-unstable nuclei by kinematic reconstruction of the decay products. This method involves the detection of the decay product of the unstable fragment in coincidence with the proton in collinear geometry, which was first applied to neutron decay measurements.[3] The decay energy can then be extracted from the relative velocity spectrum, which will exhibit two peaks that correspond to the proton emitted at 0° or 180°. The measured decay energy of these nuclei can be directly related to the mass of these proton-unstable nuclei if the decay corresponds to the ground state. In addition, the energies of excited states, if they exist, could also be extracted along with their decay widths.

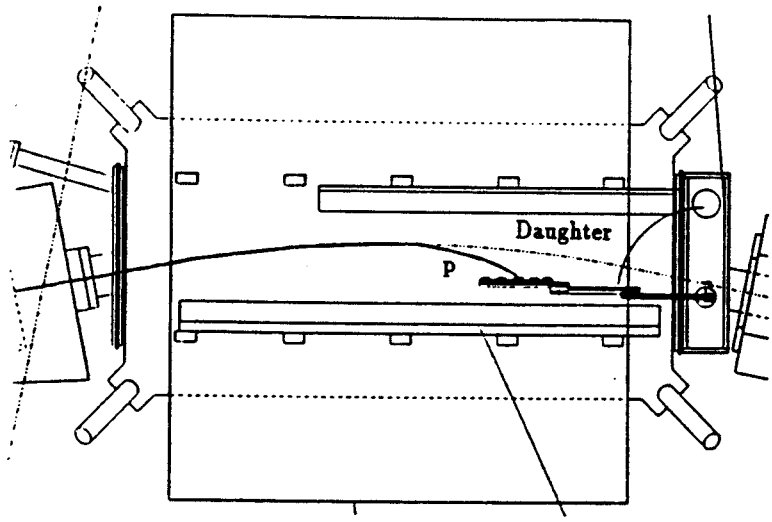

Figure 1: Schematic diagram of the location of the five pin-diode detectors inside the first A1200 dipole. Trajectories of the daughters (dot-dashed) and protons (solid) are indicated.

In a first experiment, an 8.9 mg/cm^2 thick ^{12}C target was bombarded with 70 MeV/A ^{16}O ions to produce these proton-unbound nuclei, which decay immediately into a daughter and a proton. These products are extremely forward focused and the daughter as well as the proton had to be detected at 0°. The fragments/daughters are detected and identified using the A1200 fragment separator. Due to their lower rigidity, the coincident protons are bent more and will hit the inner side of the first dipole of the A1200. Therefore, an array of 5 pin-diode detectors, each measuring 3x3 cm^2, were installed inside this dipole as shown in Figure 1. The proton identification was achieved by energy loss and time of flight measurements. The daughter and proton velocities are calculated from their time of flights.

Figure 2 shows a time of flight spectrum of ^{14}O in coincidence with protons. The real coincidences originating from the decay of ^{15}F are clearly visible compared to random coincidences from different beam bursts.

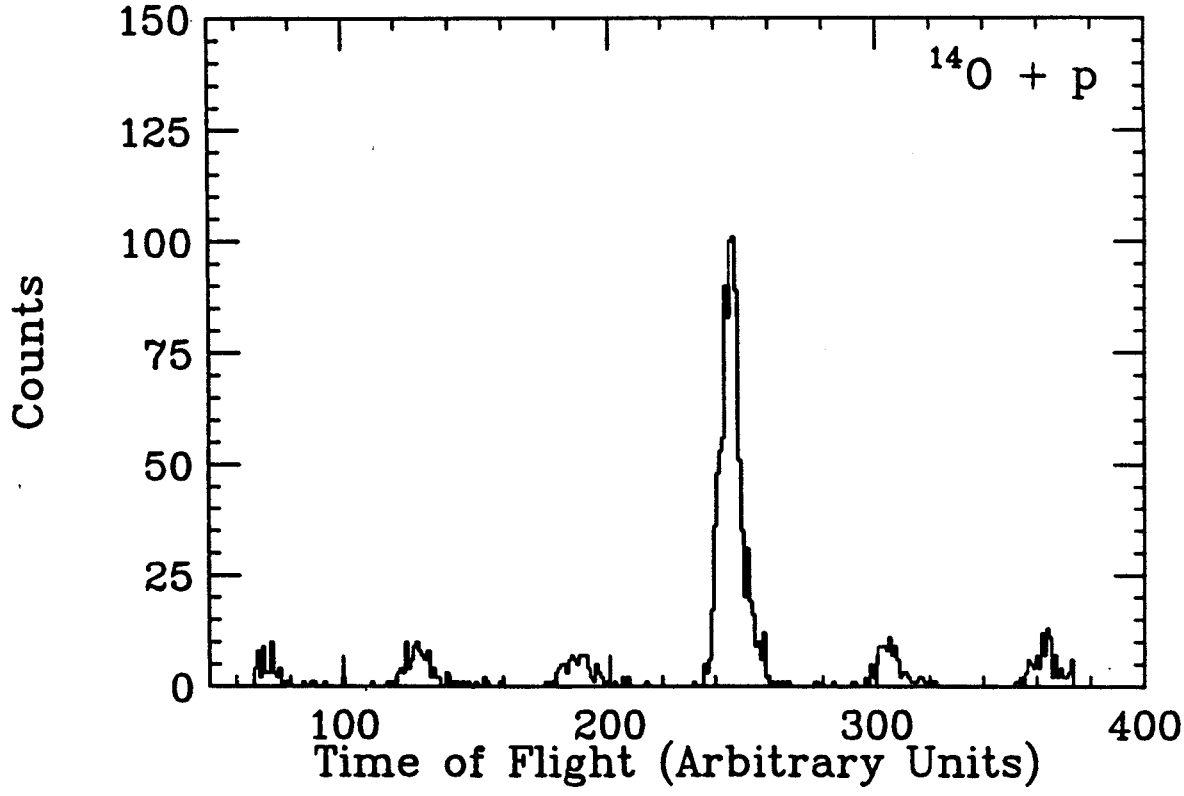

Figure 2: Time of flight spectrum of ^{14}O in coincidence with protons.

This first experiment showed the feasibility of this method. We successfully detected and identified protons inside the dipole in coincidence with daughter nuclei. However, the time resolution was not sufficient to extract a relative velocity spectrum.

Currently we are designing an improved experimental set-up in order to achieve a quantitative measurement of the mass of ^{15}F.

References

1. J. D. Robertson, J. E. Reiff, T. F. Lang, D. M. Moltz, and J. Cerny, Phys. Rev. C42, 1922 (1990).
2. R. E. Tribble, R. A. Kenefick, and R. L. Spross, Phys. Rev. C13, 50 (1976), R. G. H. Robertson, W. Benenson, E. Kashy, and D. Mueller, Phys. Rev. C13, 1018 (1976).
3. F. Deák, A. Kiss, Z. Seres, G. Caskey, A. Galonsky, and B. Remington, Nucl. Instr. Meth. A258 67 (1987).

^{32}Si LIFETIME BY IMPLANTATION

Yuming Chen, E. Kashy, B. M. Sherrill, W. Benenson, D. Bazin, D. Morrissey, and N. Orr

Measuring half-lives in the 100 to 10,000 year range has presented many difficulties. As part of the thesis research of graduate student Yuming Chen, a measurement of the ^{32}Si half-life has shown both the power and the problems of the method. By implanting a large, known number of ^{32}Si ions in an aluminum foil and measuring the activity of the sample, the half-life is easily calculated, with the uncertainty coming from the determination of the number of implanted ions and of the absolute activity. While the error in the number of ions implanted can be made very small, the measurement of the activity, in this case beta emission with an end point of 1.71 MeV, is far more difficult. The implantation depth and areal distribution and the detector response and efficiency are important. In the current measurement, we were able to measure daughter response function and efficiency directly, by implanting ^{32}P in a similar experiment. Since its half-life is well known, and its end point is also 1.71 MeV, results for ^{32}Si could be obtained without recourse to calculated efficiencies and detector response, thus eliminating a major source of uncertainty and error in the measurement.

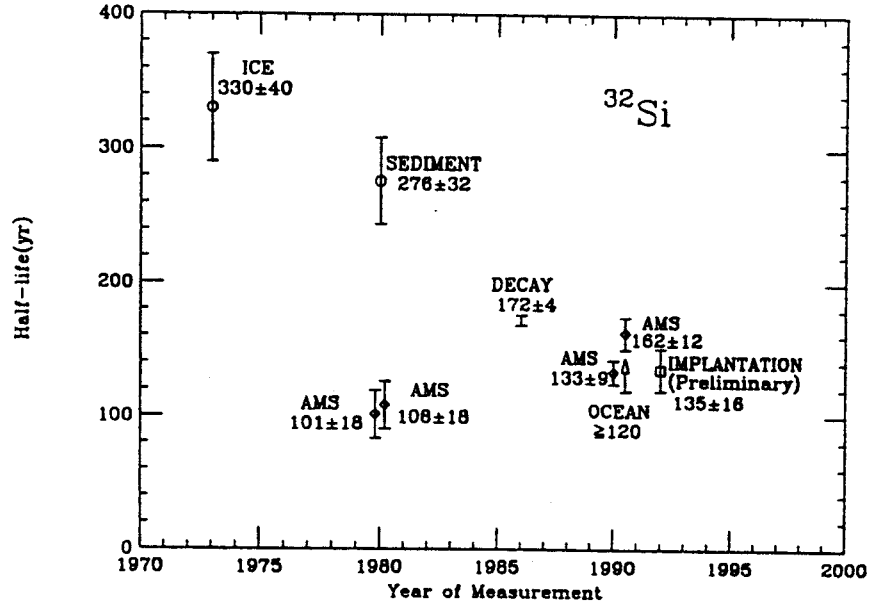

Figure 1: Summary of halflife measurements of ^{32}Si. The results are labelled by the method of measurement or the respective reservoir and by the halflife value in years.

There are a number of measurements of the ^{32}Si half-life [1], but with significant variations in results with different methods. Its cosmogenic nature has made it useful in many applications as a geological tracer. Figure 1 gives a summary of the present ^{32}Si lifetime measurements as a function of

date. The scatter in results emphasizes the need to carry out such measurement by as many different methods as possible. However, the most recent and precise data are in good agreement with each other and the present preliminary result. Now that we are well on the way to solving the problems associated with the implantation method, we plan to apply it to ^{44}Ti, ^{59}Ni and ^{60}Fe and to any other interesting cases that may arise.

Reference

1. M.S. Thomsen, J. Heinemeir, P. Hornshoj, H.L. Nielsen and N. Rud, Nucl. Phys. A534,327(1991).

STUDIES OF ISOMERIC STATE POPULATIONS OF PRODUCTS FROM INTERMEDIATE ENERGY FRAGMENTATION REACTIONS

B. M. Young, W. Bauer, D. Bazin, W. Benenson, D. J. Morrissey, N. A. Orr, R. Ronningen, B. Sherrill, M. Steiner, K. Subotic[a], M. Thoennessen, J. A. Winger, and S. J. Yennello

The projectile–like products of fragmentation reactions may be in excited states which decay immediately by gamma or particle emission. It is the secondary spectrum, consisting predominantly of fragments in their ground states, which is observed in most experiments. However, certain nuclear fragments are produced in isomeric (i.e. measurably long–lived) excited states. For nuclear fragments that have an isomeric state with a decay mode which is very different from that of the ground state, it is possible to make direct measurements of the relative populations of the two states. Studies of this type have several benefits. Since isomeric and ground states usually differ by several units of angular momentum, measurements of the relative populations of these states could provide important insight into the role of angular momentum in fragmentation reactions. If a method is devised, using fragment separators such as the A1200 at the NSCL, to create beams with a high concentration of particles in excited states, it would be possible to study reactions in which one of the reactants is in an excited state.

In 1991 and early 1992 a series of experiments were performed to measure the production rates of various fragment nuclei in their isomeric and ground states. The fragments studied were ^{26}Al, ^{24}Al, ^{38}Cl, and ^{38}K. These nuclei were produced using several beams on light targets (see table 1) at energies $E/A = 50$ — 100 MeV. A beam of fragments was produced using the A1200 fragment separator and transported to the N3 vault. The beam passed through a thin scintillator which provided a ΔE signal and time–of–flight information. This information was used to provide particle identification which allowed counting of the number of nuclei of interest, as well as determination of beam contaminants (Fig. 1).

Typical contaminations were less than 30% of the total beam. The beam was focused onto an aluminum disk approximately 30 cm in diameter and 0.1 mm thick (Fig. 2).

Particles were implanted in the disk for approximately one isomer half–life. After the implantation, the beam was turned off and the disk was rotated to position the implanted region between two 3 cm × 3 cm NaI detectors. A time histogram, with $t = 0$ corresponding to the time when the implantation stopped, was then collected for approximately one isomer half–life. After one half–life, the beam was turned on and the procedure was repeated. Analysis consisted of fitting an exponential decay curve to the time histogram to

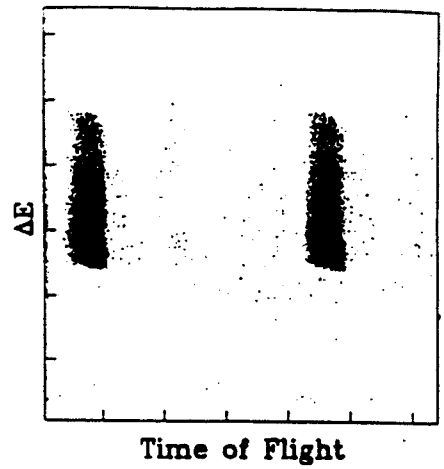

Figure 1: ΔE–TOF plot for Ar + C $\rightarrow$ ^{26}Al. Two particle groups, both of which are ^{26}Al, are shown because the timing was taken over two cycles of the cyclotron R.F.

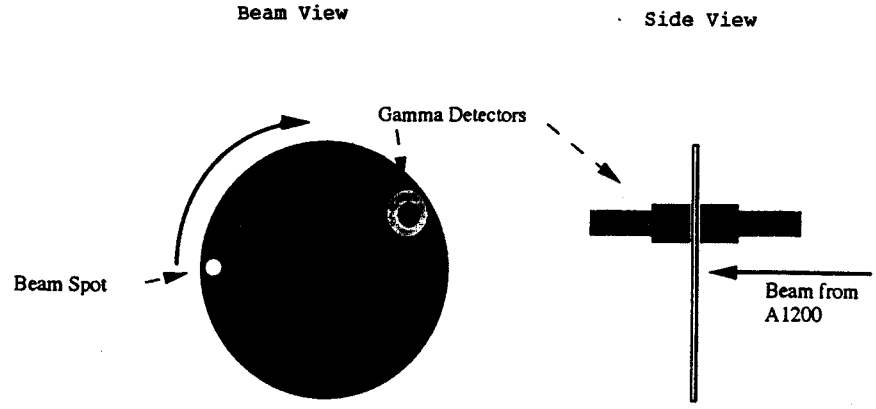

Figure 2: Diagram of experimental apparatus.

determine the number of isomers that were implanted at the moment the beam was turned off (Fig. 3).

The ratio of isomers to ground states was determined by combining this information with the total number of nuclei obtained from ΔE–TOF. The detector efficiencies were determined by performing the same procedure with a nucleus having a 100% branching ratio to a decay mode and half–life similar to the isomer of interest.

As a specific example, consider ^{26}Al. The ground state has a half–life on the order of 10^6 years, whereas the isomer decays by β^+ emission with a half–life of approximately 6 seconds. In the experiments examining the ^{26}Al isomer, the detectors, which were set up to look for the coincident 0.511 MeV gamma rays that result from the β^+ annihilation, were calibrated with a beam of ^{27}Si, which decays via β^+ emission with a half–life of approximately 4 seconds. In these experiments, the implantation and

histogram collection times were both 10 seconds.

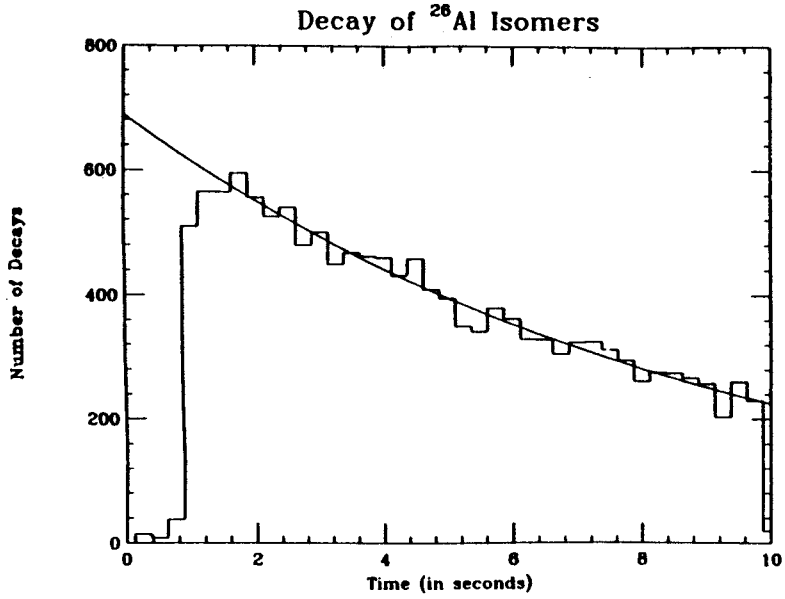

Figure 3: Time histogram of $^{26}Al^{m}$ decays. Note that for the first 1 second of the histogram there are no decays. This corresponds to the time taken for the implanted isomers to be rotated into position between the gamma ray detectors.

The experimental results are presented, along with pertinent information about the systems studied, in Table 1.

Beam/Target	E/A(MeV)	Nucleus	$J^{\pi}_{G.S.}/J^{\pi}_{iso}$	Ratio N_{iso}/N_{tot} (%)
Ar / C	65	^{26}Al	$5^{+}/0^{+}$	24 ± 1
Al / Be	100	^{26}Al	$5^{+}/0^{+}$	49 ± 2 (ref. 1)
Si / Be	80	^{26}Al	$5^{+}/0^{+}$	56 ± 3
V / Al	55	^{38}Cl	$2^{-}/5^{-}$	17 ± 3
V / Al	55	^{38}K	$3^{+}/0^{+}$	2 ± 7
Si / Be	80	^{24}Al	$4^{+}/1^{+}$	< 1

Table 1: Measured ratios of isomer yield to total yield of nuclei for intermediate energy systems.

Also included in Table 1 is the measurement of Tanihata et al.[1]. In an attempt to explain these results, the data have been compared to the model described by Gaimard and Schmidt [2]. Specifically, the technique of reference 2 is used to obtain the cross sections, excitation energies, and spins of the hot prefragments, which are then allowed to undergo statistical decay using a modified version of the CASCADE code [3,4]. This model shows significant disagreement with both the order of magnitude and the

trend of the measured results. Further theoretical work is in progress.

a. Boris Kidrich Institute, Belgrade

References

1. I. Tanihata, X. X. Bai, R. Boyd, N. Inabe, T. Kubo,C.–B. Moon, S. Shimoura, and T. Suzuki. Fourth International Conference on Nucleus– Nucleus Collisions, Kanazawa, Japan. June 1991.
2. J.–J. Gaimard and K.–H. Schmidt. Nucl. Phys. A531 (1991) 709.
3. F. Puhlhofer. Nucl. Phys. A280 (1977) 267.
4. M. N. Harakeh. Private communication.

DIFFERENCES IN HIGH ENERGY γ-RAY SPECTRA FROM THE DECAY OF ^{150}Er and ^{160}Er COMPOUND NUCLEI

E. Ramakrishnan, M. Thoennessen, J. R. Beene[a], R. L. Auble[a], C. Baktash[a], F. E. Bertrand[a], M. L. Halbert[a], D. J. Horen[a], P. E. Mueller[a], D. H. Olive[a], and R. L. Varner[a].

The observation of entrance channel effects in heavy ion fusion evaporation reactions can still not be explained, and is of high current interest. A measurement of high energy γ-rays following the fusion reaction ^{64}Ni + ^{96}Zr forming ^{160}Er at E_{ex}= 53 MeV was in disagreement with standard statistical model calculations.[1] A subsequent measurement of ^{150}Er at E_{ex}= 57 MeV formed via the reaction ^{58}Ni + ^{92}Zr reported no discrepancies of the γ-ray spectra with the statistical model.[2]

Due to these apparently contradictory observations, we studied both systems with the above mentioned reactions. The measurements were performed using the HHIRF tandem at Oak Ridge National Laboratory. The high energy γ-rays were detected with the four arrays of the Oak Ridge BaF_2 detectors, and the γ-ray multiplicity was measured with the Spin Spectrometer.[3]

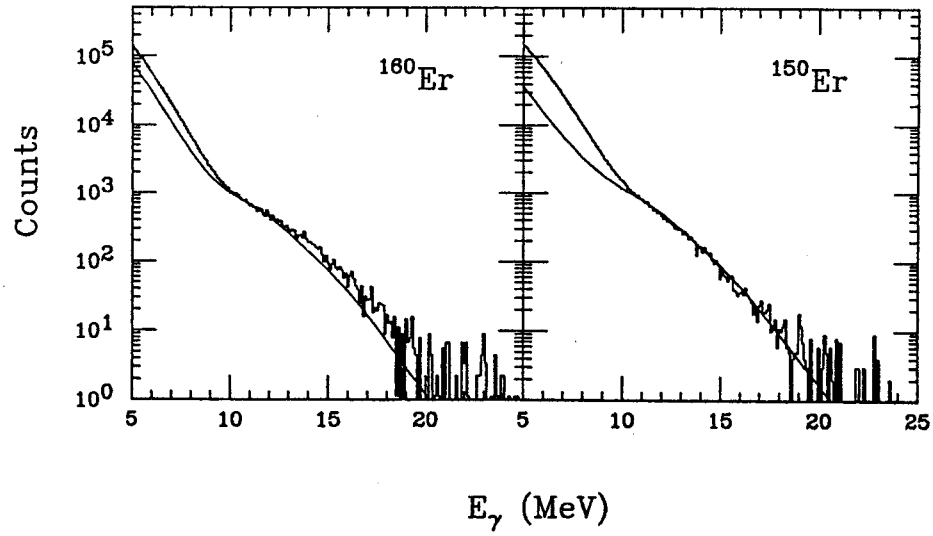

Figure 1: High energy γ-rays from the decay of ^{160}Er and ^{150}Er. The solid lines are CASCADE calculations.

Figure 1 shows the γ-ray spectra from the decay of ^{150}Er and ^{160}Er together with statistical model calculations. The data was gated on multiplicities corresponding to angular momenta of 15 - 30$\hbar$ and calculations were restricted to the same spin range. It is obvious that neither system can be described within the standard statistical model. Ref. 2 observed similar discrepancies at low γ-ray

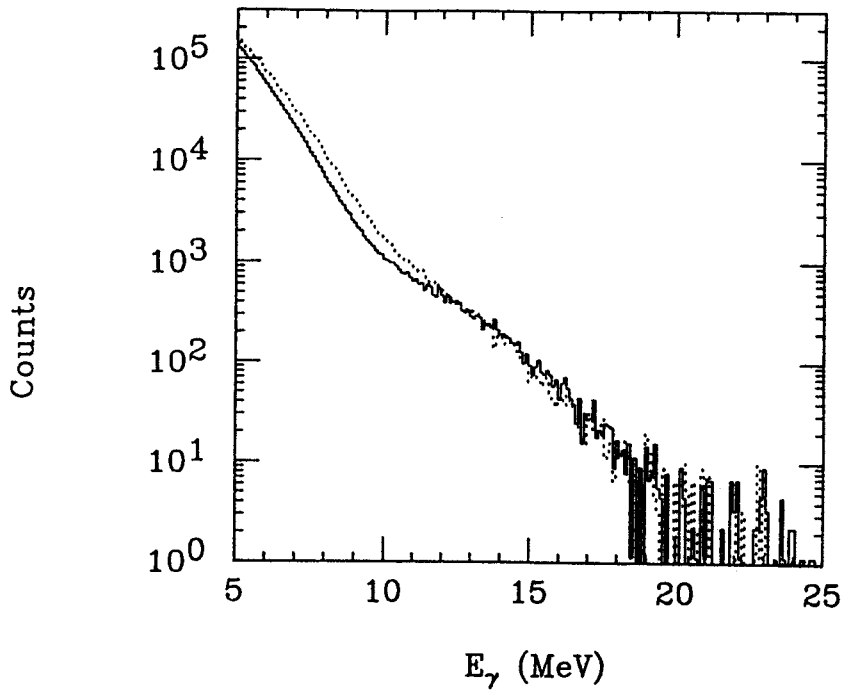

Figure 2: Comparison of the high energy γ-rays from the decay of ^{160}Er (solid) and ^{150}Er (dotted).

energies and this was attributed to contributions from deep inelastic collisions. However, ref. 2 was an inclusive measurement, whereas in the present experiment, the multiplicity gate should eliminate those contributions.

There are also differences between the experimental spectra of ^{150}Er (solid) and ^{160}Er (dotted), as shown in figure 2. This difference might be due to the fact that ^{150}Er does not decay into well know rotational evaporation residues. Almost all evaporation residues of ^{150}Er have high spin isomeric states so that the same multiplicity cut effectively gates on much higher compound nucleus angular momentum, compared to ^{160}Er. This effect should also be take into account in the calculations for ^{150}Er in figure 1. However, detailed transformations of multiplicity to spin have to be performed. This analysis of the data is currently under way.

a. Oak Ridge National Laboratory, Oak Ridge, Tennessee.

References

1. M. Thoennessen *et al.*, in "Nuclear Structure and Heavy Ion Dynamics 1990", Edited by R. R. Betts and J. J. Kolata, Institute of Physics Conference Series 109, Adam Hilger, 1991.
2. Z. M. Drebi, M. S. Kaplan, K. A. Snover, and D. P. Wells, NPL Ann. Rep., University of Washington, (1992), p.10.
3. E. Ramakrishnan, *et al.*, this report.

SEARCH FOR ENTRANCE CHANNEL EFFECTS IN EXCITED Sn NUCLEI

E. Ramakrishnan, M. Thoennessen, J. R. Beene[a], R. L. Auble[a], C. Baktash[a], F. E. Bertrand[a], M. L. Halbert[a], D. J. Horen[a], P. E. Mueller[a], D. H. Olive[a], and R. L. Varner[a].

Recent heavy ion fusion-evaporation experiments forming compound nuclei in the A = 160 mass region have show strong entrance channel effects. Large discrepancies were observed in the high energy γ-ray spectra from the decay of these rare earth nuclei following fusion reactions with ^{16}O and ^{64}Ni projectiles. The γ-ray spectra from the more asymmetric reactions were in agreement with standard statistical model calculations, whereas the γ-ray spectra from the more symmetric entrance channels could not be fitted.[1]

It had been suggested that entrance channel dependance differences in the decay of ^{156}Er was possibly due to the existence of superdeformed states in this mass region.[2] In order to test this hypothesis, we extended the measurement of high energy γ-rays to the mass region of ^{110}Sn, which is spherical in the ground state and has been measured to be spherical even at high excitation energies.[3]

The experiment was performed using the HHIRF tandem at Oak Ridge National Laboratory. Fusion reactions of ^{50}Ti + ^{60}Ni at E_{beam}= 163.0 MeV and ^{18}O + ^{92}Mo at E_{beam}= 71.6 MeV were used to form the compound nucleus ^{110}Sn at excitation energy of E_{ex}= 56.0 MeV. The high energy γ-rays were measured in five arrays of BaF_2 detectors, each consisting of 19 detectors and placed at a distance of 55 - 60 cm from target for adequate neutron separation by time of flight. The detectors covered a total solid angle of 9%. The total γ-ray multiplicity was measured with the Spin Spectrometer.

Figure 1 shows the γ-ray spectra from the decay of ^{110}Sn formed with ^{18}O (a) and ^{50}Ti (b). The spectra were gated by multiplicities corresponding to angular momenta of 15 - 30$\hbar$. Both spectra exhibit the characteristic bump between 10 and 15 MeV due to the decay of the giant dipole resonance. Statistical model calculations using the code CASCADE are shown in figure 1 as solid lines and are in excellent agreement with the data. Thus there is no evidence for entrance channel effect in this system. The extracted GDR parameters of E_{GDR} = 14.7 MeV and Γ_{GDR} = 6.5 MeV are in agreement with previous measurements in this mass region and excitation energy.[3]

This result seems to indicate that the deformation in the compound nucleus is responsible for the entrance channel effects. However, calculations using a dissipative collision model[4] suggest that the entrance channel effects can be due to significant differences in compound nucleus formation time.

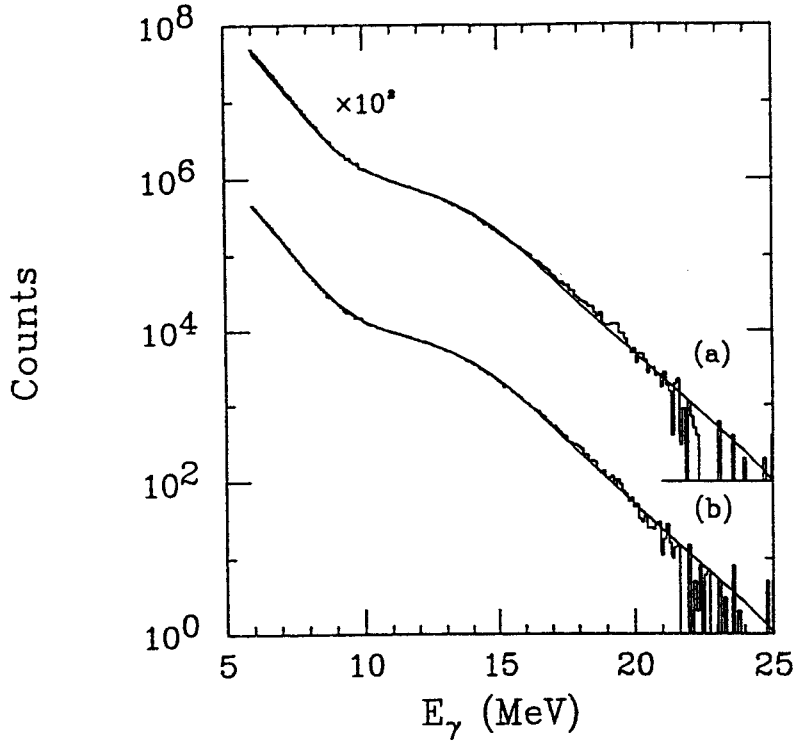

Figure 1: High energy γ-rays from the decay of ^{110}Sn formed with with ^{18}O (a) and ^{50}Ti (b). The solid lines are CASCADE calculations for the two reactions.

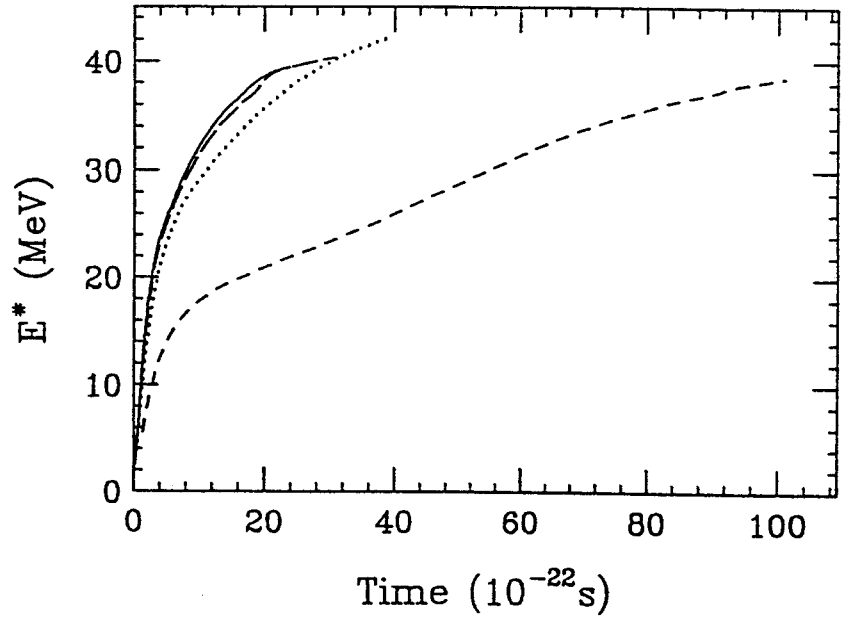

Figure 2: Evolution of excitation energy as a function of time for the reactions ^{18}O+^{92}Mo(solid), ^{50}Ni+^{60}Ti(dots), ^{16}O+^{148}Sm(long-dashed), and ^{64}Ni+^{100}Mo(short-dashed).

Figure 2 shows the equilibration of excitation energy as a function of time for the reactions $^{18}O+^{92}Mo$, $^{50}Ni+^{60}Ti$, $^{16}O+^{148}Sm$, and $^{64}Ni+^{100}Mo$. The only system that cannot be fitted with standard statistical model parameters, $^{64}Ni+^{100}Mo$, shows a large equilibration time. This large formation time may result in significant evaporation of particles and γ-rays during equilibration, thus leading to the population of different compound nuclear states. The discrepancy of the γ-ray spectra compared to statistical model calculations can then be due to both effects, (I) γ-ray emission during formation and (II) different compound nuclear population.

a. Oak Ridge National Laboratory, Oak Ridge, Tennessee.

References

1. M. Thoennessen *et al.*, in "Nuclear Structure and Heavy Ion Dynamics 1990", Edited by R. R. Betts and J. J. Kolata, Institute of Physics Conference Series 109, Adam Hilger, 1991.
2. F. L. H. Wolfs, R. V. F. Janssens, R. Holzmann, T. L. Khoo, W. C. Ma, and S. J. Sanders, Phys. Rev. C 39, 865 (1989).
3. D. R. Chakrabarty, S. Sen, M. Thoennessen, N. Alamanos, P. Paul, R. Schicker, J. Stachel, and J. J. Gaardhøje, Phys. Rev. C 36, 1886 (1987).
4. H. Feldmeier, Rep. Prog. Phys. 50, 915 (1987).

NUCLEAR DISSIPATION AND THE FEEDING OF SUPERDEFORMED BANDS

M. Thoennessen and J. R. Beene[a]

One of the main still open questions related to superdeformed bands is the feeding mechanism. Experimentally it has been determined that the population of superdeformed bands is unexpectedly large (1 - 2% of the total population) and that they are populated only over a narrow region of the highest spins of the evaporation population.[1] In most cases the high-spin limit of the evaporation residue population is determined by the competition with fission (fission cut off). A number of aspects of the feeding of superdeformed bands have been investigated theoretically,[2] but one aspect that has not been explored is how the high-spin cut off due to fission might be influenced by dynamical effects in the fission process. Recent observations[3,4] of enhanced neutron and γ-ray emission prior to fission have been explained by taking nuclear dissipation effects[5] into account; fission is slowed down due to the dissipation and this allows for additional evaporation of light particles and γ-rays prior to scission. The population distribution in mass and excitation energy of the primary fission fragments are affected by this phenomenon. On the average the fission fragments will have a lower mass and less excitation energy.

Statistical model calculations including dissipation show that also the compound nucleus populations are effected.[6] Figure 1 shows the fusion, fission and evaporation residue cross sections for the reaction ^{16}O + ^{159}Tb at E_{beam} = 160 MeV. The fission cross section distribution is shifted towards lower spin values, while the evaporation residue cross section extends to larger spins. Overall this seems to be a small effect, however superdeformed bands are populated only from the highest spin values of the evaporation residue cross section and even a small change of the population distribution can yield an important increase in the population of the superdeformed bands.

Figure 2 (a) shows the relative contribution of the evaporation cross section to the total fusion cross section of the standard calculation (dashed) compared to the calculations including dissipation mechanisms (solid). The population above 60 $\hbar$ relative to the total evaporation residue cross section increases from 8% for the standard calculation to 10% for the dissipation calculation. Above 65 $\hbar$ the evaporation residue cross section increases from 1.7% to 2.8%. Fig. 2 (b) shows the ratio of the effective total evaporation residue population calculated using dissipation and the standard calculation for spins above a given spin. For example, the population increases above 60$\hbar$ and 65$\hbar$ are 25% and 65%, respectively, as indicated by

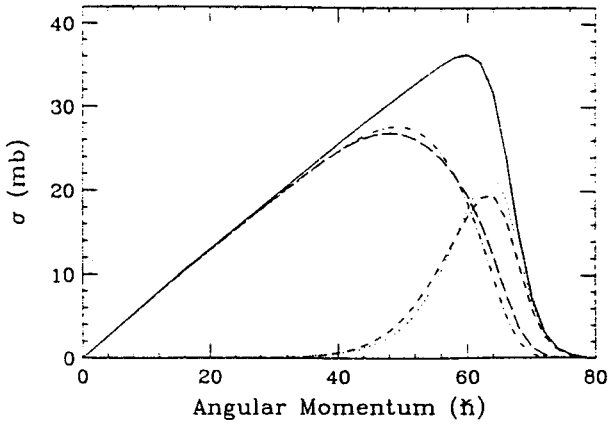

Figure 1: Spin distributions for $E_{Beam} = 160$ MeV: total fusion (solid), evaporation residues (dot-dashed) and fission (dotted) calculated with the standard statistical model and evaporation residues (long-dashed) and fission (short-dashed) calculated by including nuclear dissipation.

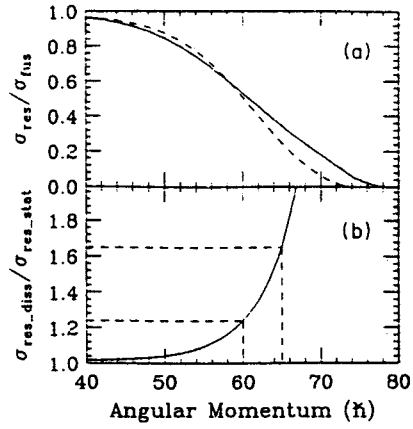

Figure 2: (a) Relative evaporation residue cross section for the standard (dashed) and dissipation (solid) calculations. (b) Ratio of dissipation to standard calculation of evaporation residue cross section population above a given spin.

the dashed lines. Our calculation with dissipation yields an enhancement above 65ħ that would implies an approximate increase of 20% in the total superdeformed population. This enhancement is purely due to the additional high-spin population that does not fission.

The present calculations show the importance of dissipation on the decay of compound nuclei. Dissipative effects can also delay the coalescence of reactants in heavy-ion fusion just as they delay fission. Thus one might be able to attribute recent observations of entrance channel dependent feeding of superdeformed bands[7] to indirect effects of dissipative dynamics.

a. Oak Ridge National Laboratory, Oak Ridge, Tennessee.

References

1. P. Taras, *et al.*, Phys. Rev. Lett. 61, 1348 (1988).
2. K. Schiffer and B. Herskind, Nucl. Phys. A520, 521c (1990).
3. D. J. Hinde, H. Ogata, M. Tanaka, T. Shimoda, N. Takahashi, A. Shinohara, S. Wakamatsu, K. Katori, and H. Okamura, Phys. Rev. C 39, 2268 (1989),
4. M. Thoennessen, D. R. Chakrabarty, M. G. Herman, R. Butsch, and P. Paul, Phys. Rev. Lett. 59, 2860 (1987).
5. P. Grangé, S. Hassani, H. A. Weidenmüller, A. Gavron, J. R. Nix, and A. J. Sierk, Phys. Rev. C 34, 209 (1986).
6. M. Thoennessen and J. R. Beene, Phys. Rev. C 45, 873 (1992).
7. G. Smith *et al.*, Phys. Rev. Lett. 68, 158 (1992).

DECOUPLED BANDS AND BAND-FORKING IN DEFORMED Re NUCLEI

Wade A. Olivier, Wen-Tsae Chou,[a] Aracelys Rios, Christine V. Hampton,
Yves M. Dardenne, Rahmat Aryaeinejad,[b] and Wm. C. McHarris

During the past few years our groups have made extensive in-beam γ-ray studies on odd-mass and odd-odd Re nuclei. Previous reports have focused primarily on the odd-odd systems, but during the past year we have discovered noteworthy new properties in some of the odd-mass nuclei, most notably in ^{175}Re. We produced ^{175}Re via the reactions, ^{165}Ho(^{16}O,6nγ) at SUNY Stony Brook, and ^{139}La(^{40}Ar,4nγ) and ^{159}Tb(^{20}Ne,4nγ) at NSCL. Four extensive rotational bands were identified in this previously uncharacterized nucleus, in essential agreement with similar bands characterized by two other groups during the past year [1,2]. These same four bands have now been seen in odd-mass Re nuclei from ^{171}Re through ^{181}Re (and also in other, mostly Ir, odd-mass nuclei in the region): I) a decoupled band based on the $h_{9/2}1/2^-[541]$ proton state, II) a highly-compressed band based on the $h_{11/2}9/2^-[514]$ state, III) a second highly-distorted, decoupled band that feeds into Band I, and IV) a relatively undistorted band based on the $d_{5/2}5/2^+$ state. These are shown in the level scheme of Fig. 1.

Nuclei in this region are very susceptible to shape-driving influences of the individual orbitals. For example, the downsloping and strongly-decoupled $\pi h_{9/2}1/2^-[541]$ state produces a strong driving force toward larger deformations, whereas the upsloping $\pi h_{11/2}9/2^-[514]$ state induces a propensity for more spherical shapes. This is demonstrated in Fig. 2, where the crossing frequencies of these bands in the series of odd-mass Re nuclei are compared with those of the even-even cores.

Perhaps the most interesting feature of the ^{175}Re level scheme is Band III, the weakly-populated, $\Delta I = 2$ band that feeds into Band I at $I = 17/2^+$. This band has been characterized in various odd-mass Re and Ir nuclei as another decoupled band with $K^\pi = 1/2^+$, based on the $\pi i_{13/2}1/2^+[660]$ state. There are, however, several serious objections to this interpretation.

First, its low population intensity. Band I is by far the most intensely populated band in all of these odd-mass systems, and at first glance it may seem peculiar that a low-K band is populated so well by heavy-ion reactions that bring in large amounts of angular momentum into the compound nucleus. In addition, we found the intensity pattern for its population in ^{175}Re to remain remarkably constant in all three reactions, which result in markedly different angular momentum distributions. The most logical explanation for this independence of the entrance channel is that decoupled states are preferentially populated by heavy-ion reactions in these nuclei, the most efficient way to cope with such large amounts of angular momentum being decoupled particles that line up with R to add to the core rotation. Such states have large coriolis coupling, and their subsequent γ-ray decay passes through similar admixed states. Thus, although Band I has a small K, it has a large i, and it is the

"yrast decoupled band." Now, if Band III did originate from the $i_{13/2}$ state, it should be populated far more strongly than it is, the reason being that it has even larger coriolis matrix elements (is more decoupled) than Band I. (The compound system lies at high enough energy to make small differences in the positions of the two states unimportant.)

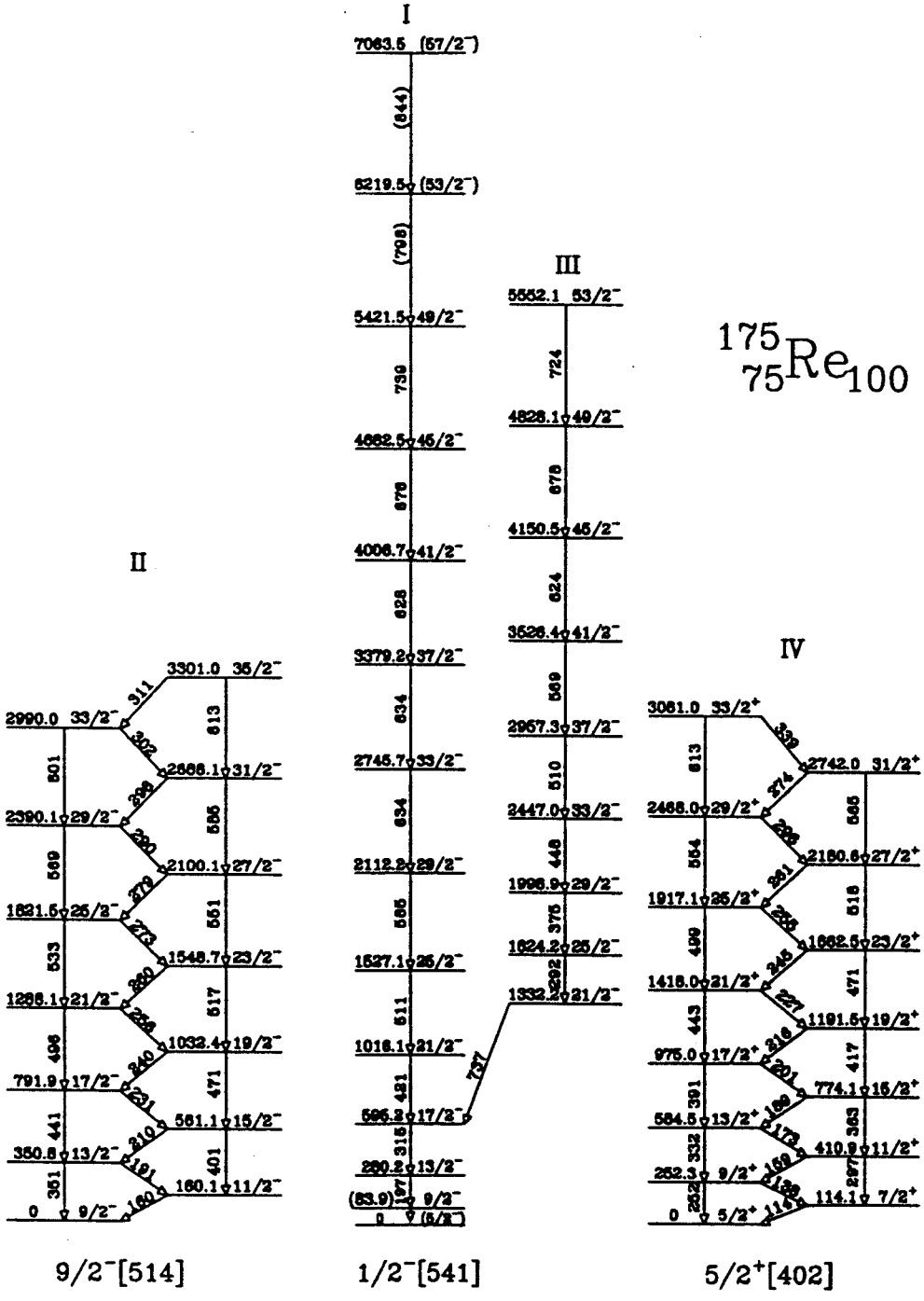

Fig. 1. Level scheme of ^{175}Re obtained from three different in-beam γ-ray reactions.

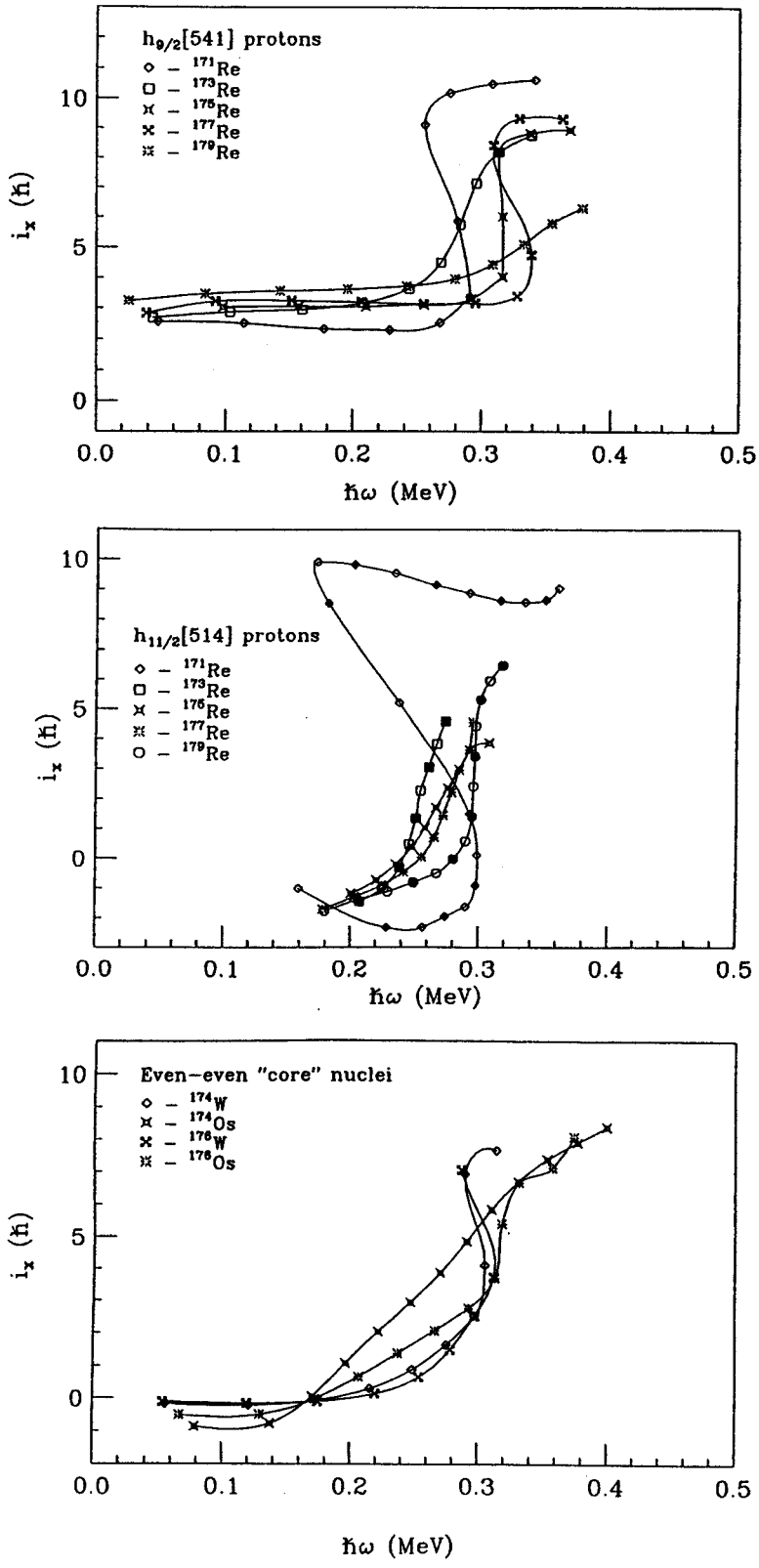

Fig. 2. Crossing frequencies of the $h_{9/2}$ and $h_{11/2}$ bands in various odd-mass Re nuclei compared with those of the even-even cores.

A second problem concerns the γ-rays connecting Band III with Band I. If Band III were the $1/2^+[660]$, these would have to be E1 transitions. Now, E1 transitions are notoriously retarded in deformed nuclei, and these particular E1's would be expected to be retarded by factors around 10^5-10^6. It is highly unlikely that an $i_{13/2}$-based Band III would decay across to Band I before reaching its base state at $13/2^+$ or lower. Thus, it seems unlikely that Band III could be such a state.

Our explanation for Band III is that it is a forked branch of Band I, most likely having a larger deformation than Band I. Wyss [3], in his total routhian calculations, has found second prolate minima for some Re nuclei in this region. If such a second minimum exists for ^{175}Re, then in the course of backbending, Band I could well fork into two pieces. The relative population of the two would naturally vary from reaction to reaction but still would be somewhat insulated from the entrance channels. A very schematic illustration of this is shown in Fig. 3.

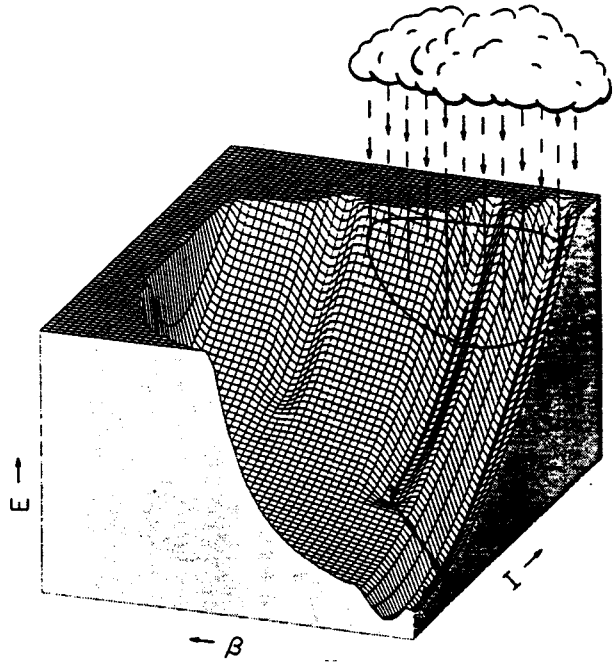

Fig. 3. Schematic illustration of a forked rotational band.

a. Present address: Brookhaven National Laboratory
b. Present address: EGG Idaho Nuclear Engineering Laboratory

References

1. H.-Q. Jin, L.L. Riedinger, C.-H. Yu, W. Nazarewicz, R. Wyss, J.-H. Zhang, C. Baktash, J.D. Garrett, N.R. Johnson, I.Y. Lee, and F.K. McGowan, Phys. Lett. B 277, 387 (1992).
2. T. Kibedi, G.D. Dracoulis, B. Fabricius, A.P. Byrne, and A.E. Stuchbery, Nucl. Phys. A539, 137 (1992).
3. R. Wyss, ORNL (private communication).

SUPERDEFORMATION IN ODD-ODD ^{132}Pr

C.V. Hampton, Aracelys Rios, W.A. Olivier, R.M. Ronningen, Wm.C. McHarris and ORNL Nuclear Structure Research group.

Additional results are presented for the reaction ^{100}Mo(^{37}Cl,5nγ)^{132}Pr, performed with the CSS γ-ray Spectrometer at HHIRF, Oak Ridge National Lab. The objective is to determine the rotational band structure of ^{132}Pr at high spin and to search for superdeformation in this nucleus. Superdeformed rotational bands (SD) have the properties of deformed prolate rotors (β= .35-.4) and appear to originate from highly deformed intruder orbitals based on at least one $i_{13/2}$ neutron.

As previously reported, the rotational bands observed with single gated, triple coincidence spectra confirm that the 160 MeV reaction populated the 5n, 4n, 3n, and possibly the 2n evaporation channels, producing ^{132,133,134,135}Pr and the p,4n and p,3n channels producing ^{132,133}Ce and the α,4n and α,3n channels for ^{129,130}La. In general, this method also confirms the three ^{132}Pr bands observed in a previous (low spin) study.[1] However, most of the transitions in this nucleus are below the 20% intensity level and there is a very evident fine structure below the 7% intensity level in the energy region between 325 and 800 keV. Multiple peaks exist, separated by about 5 keV. Since the possibility exists that these are actually multiple, low intensity bands with closely related moments of inertia from which SD transitions may arise, a double gating method was developed to better select the ^{132}Pr transitions. Events in coincidence with four major transitions (116, 130, 178, 283 keV) were scanned into a 2-D array; then selected energy gates were summed to represent each band. The negative parity, prolate shaped $\pi h_{11/2} \otimes \nu g_{7/2}$ (band 1) and the triaxial $\pi h_{11/2} \otimes \nu h_{11/2}$ (band 2) have been extended by a few energy transitions. This nucleus appears to have a very compressed energy decay scheme. It is possible that higher spin states are present within the existing structure, since many low intensity peaks can be seen in coincidence. Higher resolution is needed to verify this.

We have seen five additional energy transitions, extending the decay scheme of what had been previously referred to as a doubly decoupled band based on a $\pi h_{11/2} \otimes \nu i_{13/2}$ orbital coupling. In coincidence with this band 3, we see many transitions from band 1 and band 2. The band appears to feed into the $14^- \rightarrow 12^-$ transition from band 1 and the $17^+ \rightarrow 15^+$ transition from band 2. This indicates that the spin levels are actually much higher than previously thought and, the band may not be doubly decoupled.

A very low intensity fourth band has been found by gating on the 378 keV peak from the multiple

peak region. The coincidence peaks are regularly spaced with nearly identical intensities. This coincides with the description of a SD band for the neighboring odd-odd ^{130}La nucleus.[2] Table1 lists both bands. The energy difference between transitions (Δ) is very close. This spacing describes a nuclear shape of $\beta \approx 0.4$. Many other low intensity peaks can be seen in this multiple peak region . The potential for multiple SD peaks is evident.

Table 1: SD Band Comparison

^{132}Pr E_γ	Δ	^{130}La E_γ	Δ
		1412	
			93
		1319	
			90
		1229	
			81
1186		1148	
	87		75
1099		1073	
	76		75
1023		998	
	78		77
945		921	
	71		70
874		852	
	88		90
786		762	
	80		
706			
	88		
618			
	83		
535			
	91		
444			
	66		
378			

References

1. Shi, S., et al.,Phys. Rev. C 37 (1988) 1478.
2. Godfrey, M.J., et al., J. Phys G. 15 (1989) L163.

HIGH LYING STATES USING SINGLE NUCLEON TRANSFER REACTIONS

G. Yoo, G.M. Crawley, N. Orr, J.S. Winfield, J.E. Finck[a], S. Gales[b], Ph. Chomaz[b], I. Lhenry[b] and T. Suomijarvi[b]

Broad resonance-like structures observed in a number of single particle transfer reactions on the ^{208}Pb and ^{90}Zr region targets have been interpreted as arising from the transfer of a nucleon into a high (or a deep lying) orbit.[1,2,3] This interpretation is based on the characteristics (energy, width, strength) of the structures. However, the fact that in some cases these broad peaks have excitation energies and widths consistent with known giant quadrupole resonance states, has prompted a suggestion that these features may also result from collective excitations.[4] The single-particle explanation of these broad resonances assumes that these states are formed, as are the low lying states, by transfer of a single-particle (stripping) or the production of a single-hole (pick-up) by a one-step process. The states are broad because the single-particle states are unbound and mix with the underlying background states. On the other hand, the explanation for the collective states assumes that particle-hole pairs may be formed by transfer reactions if a target has particle or hole states in the ground state. Indeed, in a microscopic description, these particle-hole configurations correspond to a coherent sum of collective states. In principle, the cross section expected for the excitation of these collective states will be small when only one configuration is excited. However, it will be comparable to the cross section for exciting single particle (hole) states when several configurations are excited at the same time.[3]

Fortunately, the two descriptions of these peaks lead to somewhat different predictions for their excitation energy and strength when the same reaction is carried out on neighboring even-even and even-odd targets, and thus it is possible to distinguish between the two features. If the broad resonance-like peaks are single particle excitations, they should appear in the spectra of neighboring targets with one particle added or subtracted from the even-even core. There may be some shift in the excitation energy and a slight broadening of the peak because of the extra particle or hole but the total strength should be very similar for the same reaction on targets in the same mass region. Whereas, if the peaks are collective states, the cross sections should vary dramatically depending on the structure of the target ground state, on the matching conditions, and on the number of accessible configurations which can be coupled. Furthermore, a rather smooth dependence of the excitation energies of collective structures is expected. We have attempted to determine the origin of these resonance-like features by comparing the

excitation energies and Q-values for the broad peaks.[5]

The transfer reactions (^{7}Li,^{6}Li), (^{7}Li,^{6}He), (^{12}C,^{13}C) and (^{12}C,^{13}N) were carried out at a bombarding energy of 30 MeV/n using projectiles from the K500 cyclotron. The reaction products were analyzed with the S320 broad range magnetic spectrograph and detected by the focal plane detector system. In each reaction, the ejectiles were measured at the grazing angles to maximize the cross sections. The energy resolution was about 500 keV full width half maximum (FWHM) for the ^{6}Li and ^{6}He spectra, and about 1 MeV FWHM for the ^{12}C, ^{13}C and ^{13}N spectra. Six self-supporting metal foil targets, ^{89}Y, ^{90}Zr, ^{91}Zr, ^{207}Pb, ^{208}Pb, and ^{209}Bi were used.

For both the stripping and pickup cases, the spectra of the same reactions on neighboring targets were compared. In all cases, the spectra on neighboring targets were very similar and the same broad features were observed with similar strength. However the excitation energies observed for similar peaks were different for neighbouring targets in some cases.

For the set of reactions ^{90}Zr, ^{91}Zr and ^{89}Y (^{7}Li,^{6}Li), shown in Fig. 1. (a), Q-value differences for the corresponding resolved states are less than 0.5 MeV. However the excitation energies of states in the final nucleus ^{92}Zr are shifted to higher excitation energies by 1.2 to 2.0 MeV compared to those of the final nucleus ^{91}Zr or ^{90}Y. This comes from the shift of the ground state which has two neutrons in the same orbit to lower energy. Reaction Q-values for the broad peaks analyzed in the ^{208}Pb, ^{209}Bi, ^{207}Pb (^{7}Li,^{6}He) reactions (Fig. 1. (b)) are all within 0.3 MeV, while the excitation energies of states in the final nucleus ^{210}Po with two protons in the same orbit are shifted to higher energy by 1.1 to 1.5 MeV compared to those of other two final nuclei. Two neutrons in the same shell give very similar results to two protons in the same shell, as in the ^{91}Zr(^{7}Li,^{6}Li)^{92}Zr and ^{209}Bi(^{7}Li,^{6}He)^{210}Po reactions. Shell model calculations for two neutrons in the $2d_{5/2}$ state of ^{92}Zr predict a shift of the ground state to lower energy by 1.26 MeV, and a similar shift to lower energy by 1.48 MeV for two protons in the $1h_{9/2}$ state of ^{210}Po.[5,6] The results of these measurements agree with these predictions to within 0.1 MeV.

In the (^{12}C,^{13}N) reaction on the set of neighboring ^{90}Zr, ^{91}Zr and ^{89}Y targets, the Q-values of the corresponding peaks all lie within 0.5 MeV to each other, while the excitation energy of the peaks in the final nucleus ^{88}Sr with two proton holes is shifted to higher energy by 1.4 to 1.8 MeV. The peak observed at excitation energy 7.9 MeV on ^{89}Y target, which was designated as a "giant resonance-like peak" in a previous study[8], shows the characteristics of single hole state rather than giant resonance state from the

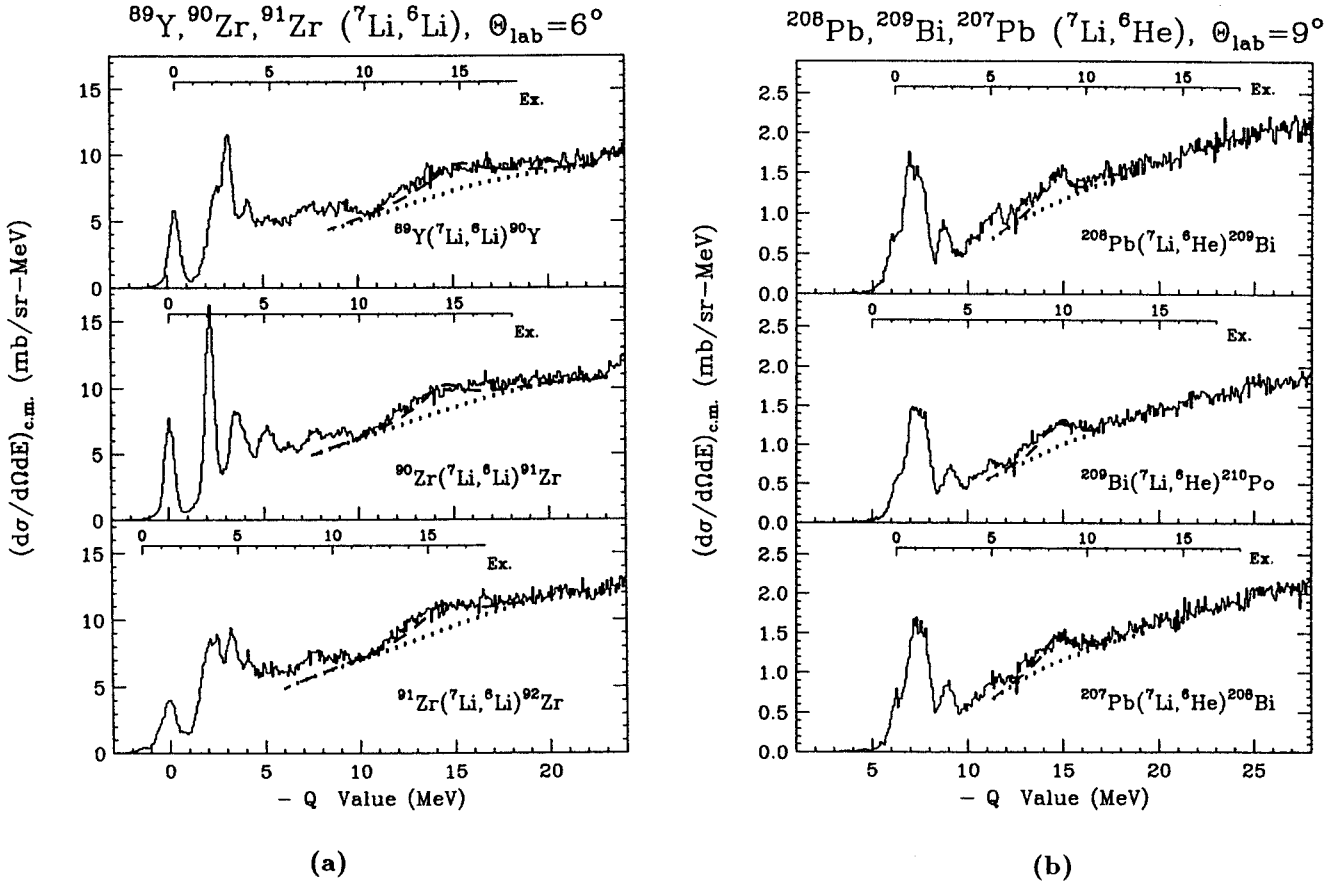

Figure 1: (a) Neutron transfer spectra on ^{90}Zr region by stripping reactions (E_{inc} = 30 MeV/n), and (b) proton transfer spectra on ^{208}Pb region by stripping reactions (E_{inc} = 30 MeV/n). Spectra are expressed as a function of reaction Q – value. The scale as a function of excitation energy is given in each graph. The dashed lines for the resonance like peaks represent the fitted curves to the experimental results, and the dotted lines represent the background assumed.

comparison of the reaction Q-values and excitation energies in the present work.[6]

Shell model calculations carried out in the lead region predicted that the single particle states, split into multiplets by an extra particle or hole in the target, are spread over 4 MeV. In this study the comparison of the shell model with experimental results agreed within a few hundred keV, and showed that the existence of an extra particle or hole outside a closed shell does not change the excitation energies significantly depending on the nuclear structure of the target ground state.[6]

Only one set of broad peaks in the reactions examined exhibited giant resonance features. They were observed at about 18 MeV in the proton pickup reaction (^{12}C,^{13}N) on Pb region targets. The peaks have similar excitation energies but different Q-values, and different strengths. In all other cases, high lying broad peaks, like the low lying states, are shifted to higher excitation energy when the ground state of the final nucleus has a closed shell or two identical particles in the same orbit. The observed shifts ranged from about 1.0 MeV for neutron pickup in the lead region to over 5 MeV for neutron pickup in the zirconium region. In addition, little variation in the strength of corresponding states was observed. These results suggest that, with the exception of one set of states, the broad peaks formed in these reactions arise from the excitations of single particle states rather than collective excitations.

a. Central Michigan University, Mt. Pleasant, Michigan

b. Institute de Physique Nucleaire, Orsay, France

References

1. S. Gales et al, Phys. Rep. 166(1988), p 125.
2. S. Fortier et al, Phys. Rev. C41(1990), p 2689.
3. C. P. Massolo et al, Phys. Rev. C34(1986), p 1256.
4. Ph. Chomaz, J. Phys. (Paris) Colloq. 47C-4(1986), p 155.
5. A. Bohr and B. Mottelson, "Nuclear Structure", Benjamin, NewYork, Vol.1(1969).
6. G. Yoo, Ph.D. Thesis, Michigan State University, unpublished, (1992).
7. S.S. Ipson et al, Nucl. Phys. A253(1975), p 189.
8. A. Stuirbrink et al, Z. Phys. A297(1980), p 307.